

Lysophosphatidylcholine inhibits membrane-associated SNARE complex disassembly

Leah Shin^a, Sunxi Wang^b, Jin-Sook Lee^a, Amanda Flack^a,
Guangzhao Mao^b, Bhanu P. Jena^{a, b, *}

^a Department of Physiology, Wayne State University School of Medicine, Detroit, MI, USA

^b Department of Chemical Engineering & Materials Science, College of Engineering, Detroit, MI, USA

Received: July 23, 2011; Accepted: August 18, 2011

Abstract

In cells, *N*-ethylmaleimide-sensitive factor (NSF) attachment protein receptors called SNAREs are involved in membrane fusion. In neurons, for example, target membrane proteins SNAP-25 and syntaxin called t-SNAREs present at the pre-synaptic membrane, and a synaptic vesicle-associated membrane protein (VAMP) or v-SNARE, is part of the conserved protein complex involved in neurotransmission. Cholesterol and LPC (L- α -lysophosphatidylcholine) are known to contribute to the negative and positive curvature respectively of membranes. In this study, using purified recombinant neuronal membrane-associated SNAREs, we demonstrate for the first time that membrane-curvature-influencing lipids profoundly influence SNARE complex disassembly. Exposure of cholesterol-associated t-SNARE and v-SNARE liposome mixtures to NSF-ATP results in dissociated vesicles. In contrast, exposure of LPC-associated t-SNARE and v-SNARE liposome mixtures to NSF-ATP, results in inhibition of t-/v-SNARE disassembly and the consequent accumulation of clustered vesicles. Similarly, exposure of isolated rat brain slices and pancreas to cholesterol or LPC, also demonstrates LPC-induced inhibition of SNARE complex disassembly. Earlier studies demonstrate a strong correlation between altered plasma LPC levels and cancer. The altered plasma LPC levels observed in various cancers may in part contribute to defects in SNARE assembly-disassembly and membrane fusion, consequently affecting protein maturation and secretion in cancer cells.

Keywords: lysophosphatidylcholine (LPC) • cholesterol • t-/v-SNARE disassembly • membrane fusion

Introduction

The assembly and disassembly of membrane proteins drive a variety of cellular activities, including membrane fusion. For example, membrane-directed self-assembly of a supramolecular ring complex [1, 2] and its subsequent disassembly [3], is required for membrane fusion and secretion in cells. Neurotransmission, and the secretion of hormones or digestive enzymes, all involve fusion of opposing bilayers. At the nerve terminal, fusion involves conserved target membrane proteins SNAP-25 and syntaxin 1A, termed t-SNAREs, and synaptic vesi-

cle-associated membrane protein VAMP2 or v-SNARE [4–6]. In the presence of Ca²⁺, when a v-SNARE-reconstituted liposome meets a t-SNARE-reconstituted liposome, SNAREs in opposing membranes interact and self-assemble in a ring, establishing continuity between the compartments [1, 2]. In the presence of ATP, this highly stable membrane-directed and self-assembled SNARE complex can undergo disassembly in the presence of the soluble NSF and ATPase [3, 7].

Cholesterol and LPC are known to contribute to the negative and positive curvature, respectively, of membranes [8, 9]. Phosphatidylcholine (PC) is a major membrane phospholipid in mammalian cells, possessing a polar phosphocholine head group and two fatty acid hydrocarbon chains. The removal of one fatty acid chains results in the production of LPC [10]. In cells, LPC originates from the enzymatic action of phospholipase A₂ (PLA₂) on PC. PLA₂ cleaves the fatty acid chain at the 2-position of the glycerol backbone of PC. Lysophosphatidylcholine is also generated from PC by the action of lecithin-cholesterol-acyl-transferase.

*Correspondence to: Bhanu P. JENA, Ph.D. (hon. doct. Mult.),
Department of Physiology,
Wayne State University School of Medicine,
5245 Scott Hall, 540 E. Canfield,
Detroit, MI 48201, USA.
Tel.: +1-313-577-1532
Fax: +1-313-993-4177
E-mail: bjena@med.wayne.edu

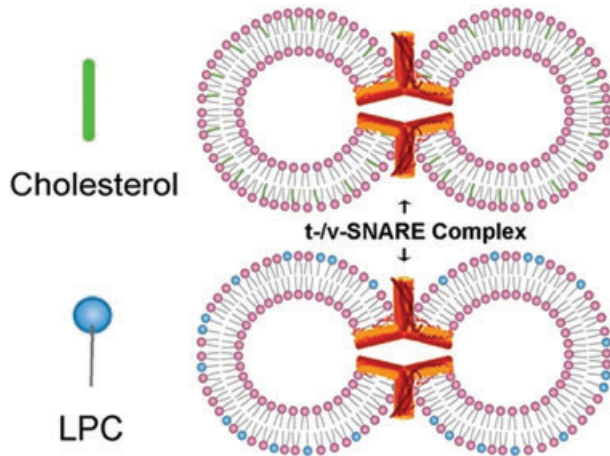


Fig. 1 Schematic drawing depicting cholesterol- and LPC-associated PC:PS vesicles reconstituted with t-SNAREs and v-SNARE, interact to form t-/v-SNARE ring complexes. In this study, the interaction between the opposing t- and v-SNARE vesicles containing either cholesterol or LPC was investigated, both in presence and absence on NSF-ATP.

Lecithin-cholesterol-acyl-transferase transfers a fatty acid from PC to cholesterol, resulting in the formation of a cholesterol ester and LPC [11]. Lysophosphatidylcholine is predominantly bound to albumin in the blood, with very small amounts of free monomolecular LPC in equilibrium. The concentration of LPC in blood plasma of healthy humans usually ranges from 200 to 400 μM [12–15]. In view of this, approximately 500 μM LPC, as elevated level of the molecule in membrane, was used in our *in vitro* liposome studies. Similarly, the exogenous exposure of 10 μM LPC to cells in our *in vivo* experiments was carried out.

Membrane-containing LPC generates larger SNARE ring complexes, where the α -helical component of the complex is little affected by NSF-ATP [16]. In contrast, cholesterol-containing membrane produces smaller SNARE ring complexes that readily disassemble in the presence of NSF-ATP [16]. In live cells, efficient t-/v-SNARE disassembly would be critical for subsequent rounds of secretory vesicle docking and fusion at the cell plasma membrane during secretion. The inhibitory effect of LPC in (NSF-ATP)-mediated t-/v-SNARE disassembly, and its possible influence on cellular secretion, was therefore hypothesized. To test this hypothesis, the association between LPC- or cholesterol-associated t-SNARE and v-SNARE liposomes in the presence of NSF-ATP, was examined using atomic force microscopy (AFM), dynamic light scattering (DLS), and X-ray diffraction measurements. Further, the disassembly of t-/v-SNAREs in isolated nerve terminals (fast secretor, msec) and exocrine pancreas (slow secretor, min.) exposed to either cholesterol or LPC was immunochemically determined. Result from the study demonstrates LPC-induced inhibition of SNARE complex disassembly both *in vitro*, and *in vivo* in live cells.

Materials and methods

Preparation of t-SNAREs, v-SNARE and NSF

N-Terminal 6xHis-tag constructs for SNAP-25 and NSF, C-terminal 6xHis-tag constructs for Syntaxin 1A and VAMP2 were generated. All four proteins were expressed with 6xHis at full length in *Escherichia coli* (*BL21DE3*) and isolated by nickel-nitrilotriacetic acid (Ni-NTA) affinity chromatography (Qiagen, Valencia, CA, USA), according to established published procedures [17–19]. Protein concentration was determined by bicinchoninic acid (BCA) assay. In the BCA assay, Cu^{2+} is reduced to Cu^{1+} by protein in an alkaline medium, and the bicinchoninic acid is then reacted with the reduced cuprous cation to produce an intense purple-coloured reaction, read using a colorimeter. The reaction product is water-soluble and exhibits a strong linear absorbance at 562 nm with increasing protein concentrations.

Preparation of proteoliposomes

All lipids were obtained from Avanti Polar Lipids (Alabaster, AL, USA). For the control group, a 5 mM lipid stock solution was prepared by mixing lipid solution in chloroform-DOPC (1,2-dioleoyl phosphatidylcholine): DOPS (1,2-dioleoyl phosphatidylserine) in 70:30 mol/mol ratios in glass test tubes. For the cholesterol group, a 5 mM lipid stock solution was prepared by mixing lipid solution in chloroform-DOPC (1,2-dioleoyl phosphatidylcholine): DOPS (1,2-dioleoyl phosphatidylserine): cholesterol in 63:27:10 mol/mol/mol ratios in glass test tubes. For the LPC group, 5 mM lipid stock solution was prepared by mixing lipid solution in chloroform-DOPC: DOPS: LPC at the molar ratio of 63:27:10 in glass test tubes. The lipid mixture was dried under gentle stream of nitrogen and resuspended in 5 mM sodium phosphate buffer, pH 7.5, by vortexing for 5 min. at room temperature. Unilamellar vesicles were formed following sonication (50 times at 10 sec./sonication), followed by extrusion using 50 nm pore-size membrane. Typically, vesicles ranging in size from 45 to 50 nm in diameter were obtained as assessed by AFM and photon correlation spectroscopy. Two sets of proteoliposomes were prepared by gently mixing either t-SNARE complex (Syntaxin-1A-His₆/SNAP-25-His₆; final concentration 25 μM) or VAMP2-His₆ (final concentration 25 μM) with liposomes [1, 13], followed by three freeze/thaw cycles to enhance protein reconstitution at the vesicles membrane (Fig. 1).

Because vesicle size influences membrane curvature and the size of the t-/v-SNARE ring complex [2], a uniform vesicle population was prepared for the entire study using minor modification of a published [2] extrusion method. Two sets of 50 nm in diameter liposomes, one set containing cholesterol and the other LPC, were reconstituted with either t-SNAREs or v-SNARE for use (Fig. 1).

Atomic force microscopy

Atomic force microscopy was performed on liposomes placed on mica surface, using minor modification of our published procedure [2, 3]. Liposomes were imaged using the Nanoscope IIIa AFM from Digital Instruments (Santa Barbara, CA, USA). Images were obtained in the 'tapping' mode in air, using aluminium-coated silicon tips with a spring constant of 40 N m^{-1} , and an imaging force of <200 pN. Images were

obtained at line frequencies of 1–2 Hz, with 256 lines per image, and constant image gains. Topographical dimensions of the lipid vesicles were analysed using the software Nanoscope IIIa4.43r8, supplied by Digital Instruments.

Wide-angle X-ray diffraction studies

X-ray diffraction was performed by a minor modification of a published procedure [20]. Fifty microlitres of 1 mM PC:PS-cholesterol or -LPC t- and v-SNARE reconstituted vesicle suspension was placed at the centre of a quartz mounted on a glass sample holder, which was placed in a Rigaku SmartLab RU2000 rotating anode X-ray diffractometer equipped with automatic data collection unit (DATASCAN) and processing software (JADE). Experiments were performed at 25°C. Samples were scanned with a rotating anode, using the nickel-filtered Cu K α line ($\lambda = 1.5418 \text{ \AA}$) operating at 40 kV and 150 mA. Diffraction patterns were recorded digitally with scan rate of 10°/min using a scintillation counter detector. The scattered X-ray intensities were evaluated as a function of scattering angle 2θ and converted into \AA units, using the formula $d = \lambda/2 \sin \theta$. Recordings were made of vesicles in solution in the 1.54–5.9 \AA diffraction range, and a broad diffraction pattern is demonstrated, spanning 2θ ranges 26.67–42.45° or d value of 2.1–3.3 \AA . The diffractogram traces exhibit a pattern typical of short-range ordering in a liquid system, indicating a multitude of contacts between interacting vesicles, majority being in the 3 \AA region. X-ray studies demonstrate larger clusters and consequently much less diffraction by the LPC vesicles compared to cholesterol. Not surprising, the average distance between cholesterol-vesicles is shorter (3.05 \AA) compared to LPC (3.33 \AA).

Light scattering measurements

Kinetics of association and dissociation of t-SNARE and v-SNARE reconstituted vesicles in solution were monitored by right angle light scattering assay with excitation and emission wavelength set at 600 nm in a Hitachi F-2000 spectrophotometer [20]. Equal volumes of t-SNARE (5 μM) and v-SNARE (5 μM) reconstituted vesicle suspension and NSF (1 $\mu\text{g/ml}$), were injected into the cuvette containing 700 μl of assay buffer (140 mM NaCl, 10 mM Hepes pH = 7.4, 2 mM CaCl $_2$) at a final lipid concentration of 100 μM at 37°C. ATP-Mg (150 μM) was added to the mixture under continuous stirring, and changes in the light scattering were continuously monitored for a 5 min. period. Values are expressed as intensities of scattered light (arbitrary units) taken continuously after addition of ATP, after which interactions between vesicles in solution reached a steady state. Student's t -test was used for comparisons between groups with significance established at $P < 0.001$.

Brain tissue preparation

Slices were prepared from rat brains according to published methods [21, 22]. Whole brain, from Sprague–Dawley rats weighing 100–150 g, was isolated and placed in ice-cold buffered sucrose solution (5 mM Hepes, pH 7.4, 0.32M sucrose), supplemented with protease inhibitor cocktail (Sigma-Aldrich, St. Louis, MO, USA). Brain slices were pre-incubated in the presence or absence of cholesterol (10 μM), LPC (10 μM), prior to incubation for 30 sec. in PBS, pH 7.4, containing 50 mM KCl. Following KCl incubation, the tissue was solubilized, protein concentration determined,

prior to SDS-PAGE, electrotransfer to nitrocellulose membrane, and immunoblot analysis using SNAP-25 antibody.

Pancreatic lobule preparation

Pancreatic lobules were prepared from Sprague–Dawley rat pancreas, and pre-incubated in the presence or absence of cholesterol (10 μM), LPC (10 μM), prior to incubation for 15 min. in PBS, pH 7.4, containing 1 μM carbamylcholine. Following incubation, the tissue was solubilized, protein concentration determined, prior to SDS-PAGE, electrotransfer to nitrocellulose membrane, and immunoblot analysis using SNAP-23 antibody.

Immunoblot analysis of SNARE complex disassembly

Quantitative assessment of SNARE complex disassembly was determined using immunochemical analysis. Isolated rat brain slices were stimulated using 30 mM KCl following exposure to 10 μM cholesterol or LPC, or vehicle (control), followed by solubilization in buffer containing 1% Triton–1% Lubrol, 5 mM ATP–EDTA in PBS. Similarly, pancreatic lobules exposed to cholesterol, LPC or vehicle (control), was stimulated using 1 μM carbamylcholine for different periods, followed by solubilization in buffer containing 1% Triton–1% Lubrol, 5 mM ATP–EDTA in PBS supplemented with protease inhibitor cocktail (Sigma-Aldrich). Interactions were stopped by addition of Laemmli reducing sample preparation buffer at room temperature and the SNARE complex formed were resolved in a 12.5% SDS-PAGE. Proteins were electrotransferred to nitrocellulose sheets for immunoblot analysis using SNAP-25 (brain) or SNAP-23 (exocrine pancreas) specific antibody (1:2000) (Alomone Labs Ltd., Jerusalem, Israel). Immunobands were visualized using a chemiluminescence detection system (Amersham BioSciences UK Ltd., Little Chalfont, Buckinghamshire, UK) and photographed using a Kodak Image Station 440. Densitometry of the immunobands were performed with the Kodak 1D Image Analysis software and is presented as relative intensities or optical density. The approximately 70 kD band is the t-/v-SNARE complex, and the lower 25 and 23 kD bands that of SNAP-25 and SNAP-23, respectively.

Results and discussion

LPC inhibits NSF–ATP induced t-/v-SNARE disassembly and vesicle aggregation

Exposure of cholesterol-associated t-SNARE and v-SNARE liposome mixtures resulted in the formation of vesicle clusters due to the interaction of t-SNARE in one vesicle interacting with v-SNARE in the opposing vesicle, as observed using AFM (Fig. 1A and B). Exposure of the vesicle clusters to NSF–ATP resulted in dissociation of the clusters due to NSF–ATP induced t-/v-SNARE complex disassembly (Fig. 2C and D). The presence of vesicles as monomers or dimers is observed following t-/v-SNARE disassembly (Fig. 2D). In contrast, exposure of LPC-associated t-SNARE and v-SNARE liposome mixtures to NSF–ATP

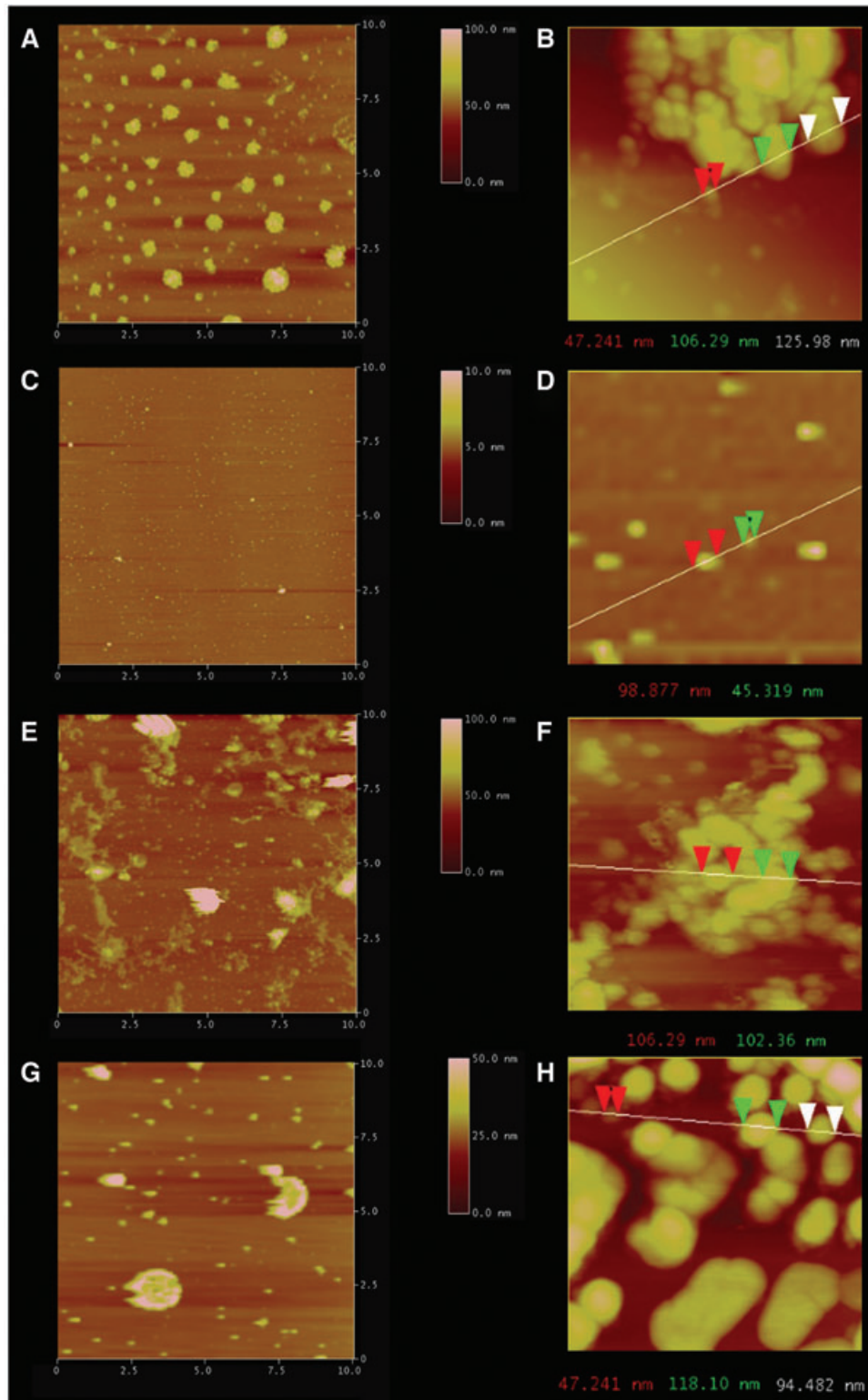
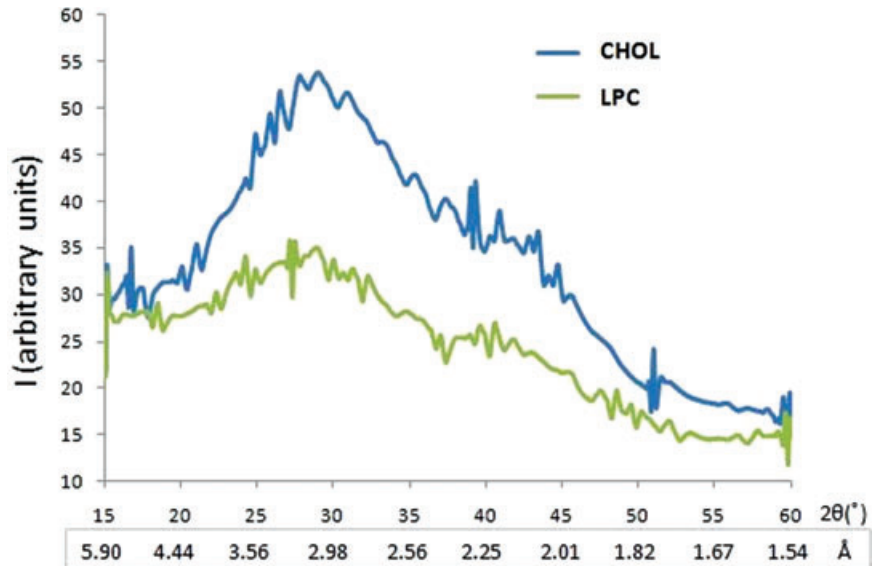


Fig. 2 Representative AFM micrographs demonstrating LPC containing t-*v*-SNARE proteoliposome complexes fail to dissociate in the presence of NSF-ATP. Exposure of cholesterol-associated t-SNARE and v-SNARE liposome mixtures (**A**, **B**), low and high magnification to NSF-ATP results in liposome dissociation as demonstrated in (**C**) at low magnification and (**D**) at higher magnification. In contrast, LPC-associated t-*v*-SNARE liposomes (**E**, **F**) remain clustered (**G**, **H**) following exposure to NSF-ATP. The left column (**A**, **C**, **E**, **G**) representing low-resolution images are all $10 \times 10 \mu\text{m}$. Similarly, the right column (**B**, **D**, **F**, **H**) representing high-resolution images are all approximately $1 \times 1 \mu\text{m}$. Note the NSF-ATP induced t-*v*-SNARE disassembly and the resultant dissociation of the cholesterol containing vesicles in (**C**) compared to (**A**), and in (**D**) compared to (**B**). As opposed to cholesterol, the NSF-ATP induced inhibition of t-*v*-SNARE disassembly and the resultant inhibition in dissociation of the LPC containing vesicles in (**G**) compared to (**E**), and in (**H**) compared to (**F**), is demonstrated.

Fig. 3 Wide-angle X-ray diffraction pattern of interacting t- and v-SNARE-reconstituted lipid vesicles, with the vesicle membrane containing either cholesterol (CHOL) or lysophosphatidylcholine (LPC). Diffraction profiles of a mixture of 50 nm in diameter t-SNARE and v-SNARE reconstituted PC:PS vesicles either containing cholesterol CHOL or LPC. Note as a consequence of clustering of LPC-containing vesicles, the diffraction is significantly lower (green peak) compared to CHOL-containing vesicles (blue peak). Interestingly, the distance between interacting t-SNARE and v-SNARE vesicles is closer between the CHOL populations (3.05 Å) compared to LPC (3.33 Å).



resulted in little or no NSF-ATP induced disassembly, and consequently the accumulation of vesicles in clusters (Fig. 2E–H).

Reduced X-ray diffraction by LPC-associated t-/v-SNARE liposomes

To further determine the influence of LPC and cholesterol on the interaction between t-SNARE and v-SNARE vesicles, X-ray diffraction studies were performed (Fig. 3). Recordings were made of vesicles in solution in the 1.54–5.9 Å diffraction range, and a broad diffraction pattern was demonstrated, spanning 2θ ranges 26.67–42.45° or d values of 2.1–3.3 Å. The diffractogram trace exhibits a pattern typical of short-range ordering in a liquid system, indicating a multitude of contacts between interacting vesicles, the majority being in the 3 Å region. In agreement with our AFM studies, X-ray studies demonstrate larger clusters and consequently much less diffraction by the LPC vesicles compared to CHOL (Fig. 3). The distance however between vesicles is closer in the CHOL population (3.05 Å) than in the LPC population (3.33 Å).

DLS demonstrates LPC inhibits t-/v-SNARE disassembly by NSF-ATP

Dissociated vesicles in suspension scatter more light than the same vesicles present in aggregates or clusters. Dynamic light scattering experiments performed on cholesterol-associated and LPC-associated t-SNARE and v-SNARE liposome mixtures in the presence of NSF-ATP, further confirm our AFM and X-ray diffraction studies (Figs 2 and 3). Dynamic light scattering studies demonstrate a total abrogation of NSF-ATP induced dissociation

of LPC-associated t-/v-SNARE liposome complexes, in contrast to CHOL-associated t-/v-SNARE vesicles (Fig. 4A). Interestingly, both the potency and efficacy of t-/v-SNARE disassembly is impaired in presence of LPC. Note the dissociation of cholesterol-associated t-/v-SNARE vesicles occurs with rate constant $k = 0.03 \text{ sec}^{-1}$ (Fig. 4B), and a slow dissociation constant of $k = 0.01 \text{ sec}^{-1}$ in LPC vesicles (Fig. 4C).

LPC inhibits t-/v-SNARE disassembly in cells

To further determine the role of cholesterol and LPC on t-/v-SNARE complex disassembly at the nerve terminal, isolated rat brain slices exposure to cholesterol, LPC or vehicle (control) were used. The brain tissue was stimulated using 150 mM KCl, followed by immunoblot analysis. It has been demonstrated that v-SNARE and t-SNAREs form an SDS-resistant complex, and NSF binds to the complex in presence of ATP (NSF-ATP) [23]. In the presence of ATP-EDTA, SNARE antibody is able to immunoprecipitate this stable NSF-SNARE complex [23]. In this study, stimulated brain slices demonstrated an inhibition of t-/v-SNARE complex disassembly in presence of LPC, further confirming AFM, X-ray and DLS experiments (Fig. 4D). These results suggest that in presence of LPC, once v-SNARE associated secretory vesicles interact with t-SNARE membrane to form the t-/v-SNARE ring complex and establish continuity, the complex fails to disassemble, resulting in an inhibition of subsequent rounds of vesicle docking and fusion. To further test this hypothesis in live cells, the experiment was repeated using exocrine pancreas. Following incubation in LPC, CHOL or vehicle, when stimulated exocrine pancreas were examined by immunoblot analysis using SNAP-23 specific antibody (Fig. 4D), results further confirmed the inhibitory effect of LPC on

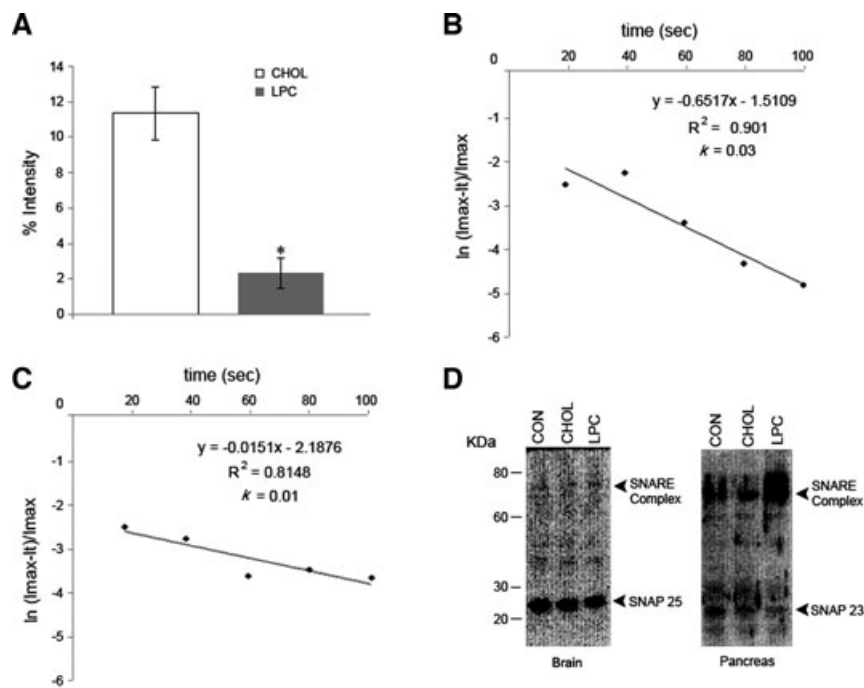


Fig. 4 SNARE complexes in the presence of LPC fail to disassemble. **(A)** Real-time dynamic light scattering (DLS) profiles on cholesterol-associated (CHOL) and LPC-associated t-*v*-SNARE liposomes in presence of NSF-ATP. There is no appreciable dissociation of the LPC vesicles, in contrast to a rapid ATP-dependent dissociation of CHOL vesicles ($P < 0.001$). **(B)** Note the dissociation of cholesterol-associated t-*v*-SNARE vesicles occurs with rate constant $k = 0.03 \text{ sec}^{-1}$, and **(C)** a slow dissociation in LPC vesicles ($k = 0.01 \text{ sec}^{-1}$). **(D)** Following KCl stimulation, isolated brain slices pre-incubated in CHOL, LPC or vehicle (CON) are solubilized in buffer containing ATP-EDTA, and 10 mg of protein resolved by SDS-PAGE, followed by immunoblot analysis using SNAP-25-specific antibody, negligible disassembly of the t-*v*-SNARE complex is demonstrated in brain tissue pre-incubated in LPC, as opposed to the control (CON) or CHOL. Similarly, exocrine pancreas pre-incubated in LPC, demonstrate reduced disassembly of the t-*v*-SNARE complex following stimulation of secretion using 1 mM carbamylcholine.

SNARE complex disassembly in live cells. These results are in agreement with earlier findings supporting LPC to be a membrane fusion inhibitor [24].

Earlier studies using AFM and circular dichroism spectroscopy [16] demonstrate that PC:PS liposomes containing LPC generate larger SNARE ring complexes, where the α -helical component of the complex is little affected by NSF-ATP. In contrast, cholesterol-containing liposomes produce smaller SNARE ring complexes similar to what is observed in control groups of plain PC:PS vesicles, that readily disassembles in the presence of NSF-ATP [16]. Previous studies implicate cholesterol's role in membrane fusion to be indirect, centred on SNARE formation through cholesterol binding to synaptophysin, a calcium- and cholesterol-dependent vesicle associated protein which forms a complex with synaptobrevin or VAMP, subsequently facilitating *v*-SNARE interaction with t-SNAREs [25]. In the present *in vitro* liposome study, no synaptophysin is present to influence such interactions of cholesterol with SNAREs. Furthermore, results from earlier studies [22] demonstrate no change in t-*v*-SNARE ring complex size or shape in SNARE-associated liposomes containing membrane cholesterol.

In this study, we report for the first time that membrane LPC inhibits SNARE complex disassembly, supporting direct lipid-protein interactions to enable differential modulation of membrane fusion and secretion in cells. Modulating the concentration and distribution of such non-bilayer lipids at various membranes, could regulate the degree and rate of membrane fusion and membrane-directed SNARE complex assembly-disassembly. Cells with

higher membrane-cholesterol levels, would promote membrane fusion while cells with increased membrane LPC content would facilitate secretory event longevity by inhibiting SNARE-complex disassembly. However, efficient t-*v*-SNARE disassembly would be critical for subsequent rounds of secretory vesicle docking and fusion at the cell plasma membrane during secretion. Studies demonstrate that ras-transformed cell lines have a higher PC-turnover and a higher consumption of LPC than normal cells [26]. Also, there are reports suggesting that PC hydrolysis is a ras target during growth factor initiated mitogenic signalling [27]. Correspondingly, studies have demonstrated a strong correlation between altered plasma LPC levels and cancer [28, 29]. Hence, the altered plasma LPC levels observed in various cancers may result in defects in SNARE assembly-disassembly and membrane fusion, consequently affecting protein maturation and secretion in cancer cells. A decrease in membrane LPC would result in rapid t-*v*-SNARE assembly-disassembly, and membrane fusion. On the contrary, an increase in membrane LPC levels would greatly slow-down t-*v*-SNARE disassembly, and consequently membrane fusion kinetics. Because LPC is a naturally occurring lipid found in membranes, and its levels are tightly regulated, it may serve among other things, a natural modulator of NSF activity. It is of interest to note that, whereas NSF is an ATPase [30] behaving as a right-handed molecular motor [31] to disassemble t-*v*-SNAREs; ATP synthase [32] is a left-handed molecular motor [33] involved in the generation of ATP in the mitochondria, and requires LPC for its multi-complex integrity.

In summary, this study demonstrates that in presence of membrane LPC, SNARE complex disassembly is inhibited, both *in vitro* in artificial proteoliposomes, and *in vivo* in live cells. This inhibition may result from the way t-/v-SNARE complexes assemble in LPC containing liposomes, or the result of a direct inhibition of NSF ATPase activity by membrane LPC. Further studies are therefore required to fully understand this inhibition of t-/v-SNARE disassembly by LPC.

Acknowledgements

This work is supported by grants from NIH and WSU (B.P.J.), and NSF MRI grants (G.M.).

References

1. **Cho SJ, Kelly M, Rognien KT, et al.** SNAREs in opposing bilayers interact in a circular array to form conducting pores. *Biophys J.* 2002; 83: 2522–7.
2. **Cho WJ, Jeremic A, Jena BP.** Size of supramolecular SNARE complex: membrane-directed self-assembly. *J Am Chem Soc.* 2005; 127: 10156–7.
3. **Jeremic A, Quinn AS, Cho WJ, et al.** Energy-dependent disassembly of self-assembled SNARE complex: observation at nanometer resolution using atomic force microscopy. *J Am Chem Soc.* 2006; 128: 26–7.
4. **Oyler GA, Higgins GA, Hart RA, et al.** The identification of a novel synaptosomal-associated protein, SNAP-25, differentially expressed by neuronal subpopulations. *J Cell Biol.* 1989; 109: 3039–52.
5. **Bennett K, Calakos N, Scheller RH.** Syntaxin: a synaptic protein implicated in docking of synaptic vesicles at presynaptic active zones. *Science.* 1992; 257: 255–9.
6. **Trimble WS, Cowam DM, Scheller RH.** VAMP-1: a synaptic vesicle-associated integral membrane protein. *Proc Natl Acad Sci USA.* 1988; 85: 4538–42.
7. **Cook JD, Cho WJ, Stemmler TL, et al.** Circular dichroism (CD) spectroscopy of the assembly and disassembly of SNAREs: the proteins involved in membrane fusion in cells. *Chem Phys Lett.* 2008; 462: 6–9.
8. **McMahon HT, Gallop JL.** Membrane curvature and mechanisms of dynamic cell membrane remodelling. *Nature.* 2005; 438: 590–6.
9. **Chernomordik L.** Non-bilayer lipids and biological fusion intermediates. *Chem Phys Lipids.* 1996; 81: 203–13.
10. **Berdel WE, Von Hoff DD, Unger C, et al.** Ether lipid derivatives: antineoplastic activity *in vitro* and the structure-activity relationship. *Lipids.* 1986; 21: 301–4.
11. **Sekas G, Patton GM, Lincoln EC, et al.** Origin of plasma lysophosphatidylcholine: evidence for direct hepatic secretion in the rat. *J Lab Clin Med.* 1985; 105: 190–4.
12. **Raffelt K, Moka D, Sullentrop F, et al.** Systemic alterations in phospholipid concentrations of blood plasma in patients with thyroid carcinoma: an *in vitro* ³¹P high-resolution NMR study. *NMR Biomed.* 2000; 13: 8–13.
13. **Takatera A, Takeuchi A, Saiki K, et al.** Quantification of lysophosphatidylcholines and phosphatidylcholines using liquid chromatography-tandem mass spectrometry in neonatal serum. *J Chromatogr B Analyt Technol Biomed Life Sci.* 2006; 838: 31–6.
14. **Kuliszkiewicz-Janus M, Janus W, Baczynski S.** Application of ³¹P NMR spectroscopy in clinical analysis of changes of serum phospholipids in leukemia, lymphoma and some other non-haematological cancers. *Anticancer Res.* 1996; 16: 1587–94.
15. **Kuliszkiewicz-Janus M, Tuz MA, Baczynski S.** Application of ³¹P MRS to the analysis of phospholipid changes in plasma of patients with acute leukemia. *Biochim Biophys Acta.* 2005; 1737: 11–5.
16. **Shin L, Cho WJ, Cook JD, et al.** Membrane lipids influence protein complex assembly-disassembly. *J Am Chem Soc.* 2010; 132: 5596–7.
17. **Söllner T, Whiteheart SW, Brunner M, et al.** SNAP receptors implicated in vesicle targeting and fusion. *Nature.* 1993; 362: 318–24.
18. **Söllner T, Bennett M, Whiteheart SW, et al.** A protein assembly-disassembly pathway *in vitro* that may correspond to sequential steps of synaptic vesicle docking, activation, and fusion. *Cell.* 1993; 75: 409–18.
19. **Sogaard M, Tani K, Ye RR, et al.** A rab protein is required for the assembly of SNARE complexes in the docking of transport vesicles. *Cell.* 1994; 78: 937–48.
20. **Jeremic A, Kelly M, Cho JA, et al.** Calcium drives fusion of SNARE-apposed bilayers. *Cell Biol Int.* 2004; 28: 19–31.
21. **Cho WJ, Jeremic A, Rognien KT, et al.** Structure, isolation, composition and reconstitution of the neuronal fusion pore. *Cell Biol Int.* 2004; 28: 699–708.
22. **Cho WJ, Jeremic A, Jin H, et al.** Neuronal fusion pore assembly requires membrane cholesterol. *Cell Biol Int.* 2007; 31: 1301–8.
23. **Jeong E-H, Webster P, Khuong CQ, et al.** The native membrane fusion machinery in cells. *Cell Biol Int.* 1998; 22: 657–70.
24. **Stiasny K, Heinz FX.** Differences in the postfusion confirmations of full-length and truncated class II fusion protein E of tick-borne encephalitis virus. *J Virol.* 2004; 78: 8536–42.
25. **Mitter D, Reisinger C, Hinz B, et al.** The synaptophysin/synaptobrevin interaction

Authors' contributions

BPJ designed the research and wrote the paper. LS prepared the t-/v-SNARE reconstituted liposomes, and performed the *in vivo* assays using pancreas and brain tissue. SW performed the AFM and X-ray studies. JSL and AF, isolated liposome, calculated the kinetics of vesicle dissociation, and participated in the liposome X-ray studies. GM helped in X-ray analysis, and critical reading of the manuscript.

Conflict of interest

The authors declare no competing financial interests.

- critically depends on the cholesterol content. *J Neurochem*. 2003; 84: 35–42.
26. **Baburina I, Jackowski S.** Cellular responses to excess phospholipid. *J Biol Chem*. 1999; 274: 9400–8.
 27. **Cai H, Erhardt P, Szeberenyi J, et al.** Hydrolysis of phosphatidylcholine is stimulated by Ras proteins during mitogenic signal transduction. *Mol Cell Biol*. 1992; 12: 5329–35.
 28. **Kuliszkiewicz-Janus M, Tuz MA, Baczynski S.** Application of ^{31}P MRS to the analysis of phospholipid changes in plasma of patients with acute leukemia. *Biochim Biophys Acta*. 2005; 1737: 11–5.
 29. **Sullentrop F, Moka D, Neubauer S, et al.** ^{31}P NMR spectroscopy of blood plasma: determination and quantification of phospholipid classes in patients with renal cell carcinoma. *NMR Biomed*. 2002; 15: 60–8.
 30. **Malhotra V, Orci L, Glick B, et al.** Role of an *N*-ethylmaleimide-sensitive transport component in promoting fusion of transport vesicles with cisternae of the Golgi stack. *Cell* 1988; 54: 221–7.
 31. **Cho WJ, Jena BP.** *N*-ethylmaleimide sensitive factor is a right-handed molecular motor. *J Biomed Nanotech*. 2007; 3: 209–11.
 32. **Walker JE, Runswick MJ, Poulter L.** ATP synthase from bovine mitochondria. The characterization and sequence analysis of tow membrane-associated sub-unit and of the corresponding cDNAs. *J Mol Biol*. 1987; 197: 89–100.
 33. **Ueno H, Suzuki T, Kinoshita K, et al.** ATP-driven stepwise rotation of F_0F_1 -ATP synthase. *Proc Natl Acad Sci USA*. 2005; 102: 1333–8.